THE JOURNAL OF PHYSICAL CHEMISTRY B

Article

pubs.acs.org/JPCB

Local Structures of Methanol–Water Binary Solutions Studied by Soft X-ray Absorption Spectroscopy

Masanari Nagasaka,[†,‡] Kenji Mochizuki,[‡] Valentin Leloup,[†] and Nobuhiro Kosugi*[,†,‡]

[†]The Institute for Molecular Science, Myodaiji, Okazaki 444-8585, Japan

[‡]The Graduate University for Advanced Studies, Myodaiji, Okazaki 444-8585, Japan

ABSTRACT: Liquid methanol shows one- and two-dimensional (1D/2D) hydrogen bond (HB) networks, and liquid water shows three-dimensional (3D) HB networks. We have clearly found three different local structures around the methyl group of methanol–water binary solutions $(CH_3OH)_X(H_2O)_{1-X}$ at different concentrations in C K-edge soft X-ray absorption spectroscopy (XAS). With the help of molecular dynamics simulations, we have discussed the concentration dependence of the hydrophobic interaction at the methyl group in the C K-edge XAS spectra. In the methanol-rich region I ($1.0 > X > 0.7$), a small amount of water molecules exists separately around dominant 1D/2D HB networks of methanol clusters. In the region II ($0.7 > X > 0.3$), the hydrophobic interaction of the methyl group is dominant due to the increase of mixed methanol–water 3D network structures. In the water-rich region III ($0.3 > X > 0.05$), methanol molecules are separately embedded in dominant 3D HB networks of water. On the other hand, the pre-edge feature in the O K-edge XAS shows almost linear concentration dependence. It means the HB interaction between methanol and water is almost the same as that of water–water and of methanol–methanol.

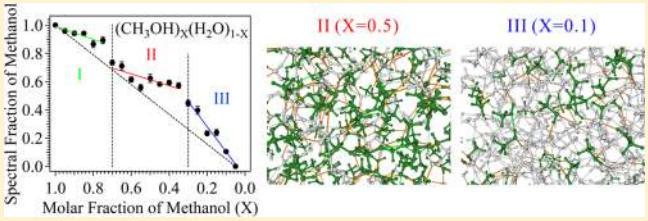

1. INTRODUCTION

It is known that methanol–water binary solutions show smaller entropy than expected in an ideal solution of randomly mixed molecules[1] and show a nonlinear profile in viscosity as changing the mixing ratio.[2] These characteristics have been discussed by using clathrate-like structure models of methanol molecules with surrounding water molecules and with hydrophobic interactions between methyl groups.[1] However, a consistent picture of the microscopic structure of methanol–water binary solutions is not yet established.

The oxygen atom in a water molecule has two hydrogen-donating ("donor") sites and two hydrogen-accepting ("acceptor") sites, and liquid water forms tetrahedrally coordinated three-dimensional (3D) hydrogen bond (HB) networks.[3] On the other hand, a methanol molecule has one donor and one or two acceptor sites due to the replacement of one donor site by a hydrophobic methyl group, and liquid methanol forms one- and two-dimensional (1D/2D) HB networks, such as chain and ring structures.[4−9] In the neutron diffraction experiments of methanol–water binary solutions,[10−12] it is found that 3D HB networks of methanol–water mixtures are formed by hydrophilic and hydrophobic interactions between water and methanol molecules. Dixit et al. measured neutron diffraction at $X = 0.7$ in the methanol–water binary solutions $(CH_3OH)_X(H_2O)_{1-X}$[11] and revealed that the distance between methyl groups of methanol molecules becomes closer by adding water molecules.

The interaction between methanol and water molecules in the binary solution was studied by nuclear magnetic resonance,[13] mass spectrometry,[14] Rayleigh scattering,[15] and dielectric relaxation methods.[16] Takamuku et al. measured the number of water molecules per 6 methanol molecules as a function of the methanol molar fraction by the mass spectrometry of methanol–water liquid microjets[14] and found three different dependences with the borders at $X = 0.7$ and $X = 0.3$. They proposed that the chain structures of methanol clusters are dominant at $X > 0.7$, the tetrahedral-like water clusters gradually evolve at $0.7 > X > 0.3$, and the water cluster is a main species at $0.3 > X > 0.0$.

The interaction in the binary solution was also investigated by vibrational spectroscopies: infrared spectroscopy[17−24] and Raman spectroscopy.[22,25−28] Dixit et al. found nonlinear profiles of the C–O stretching vibration in the Raman spectroscopy when decreasing the methanol molar fraction,[27] in which the behavior of the energy shifts changes at $X = 0.70$ and $X = 0.25$. They proposed different local structures: in the region $X > 0.7$, water molecules connect the terminal of the methanol chain and the chain structure is preserved; in the region $0.7 > X > 0.25$, the methanol chain is broken by adding water molecules; in the region $0.25 > X > 0.05$, the hydration structure of methanol molecules is formed.

The structure of liquid methanol and methanol–water binary solutions has been investigated theoretically by using molecular dynamics (MD)[29−43] and Monte Carlo simulations.[44−49] In the methanol-rich condition, the 1D/2D HB network structure of methanol clusters is not strongly influenced by water

Received: September 13, 2013
Revised: March 4, 2014
Published: April 3, 2014

   dx.doi.org/10.1021/jp4091602 | J. Phys. Chem. B 2014, 118, 4388−4396

molecules.[32] As the mixing ratio of water increases, the HB networks of both water and methanol molecules grow to be mixed with each other.[38−40,46,48] When the mixing ratio of water is high, the 3D hydration shell is formed around methanol molecules.[41,43,45]

Although methanol−water binary solutions have been studied experimentally and theoretically as described above, microscopic structures of methanol−water mixtures, such as nearest-neighbor interactions, have not yet been known in detail. Soft X-ray absorption spectroscopy (XAS) is an element-selective method to investigate local structures of liquid and aqueous solutions. The structure of liquid water was extensively studied by the O K-edge XAS.[50−52] Because the X-ray absorption process occurs within a few femtoseconds, XAS enables us to investigate the HB interaction of liquid water before the geometrical rearrangement. The hydration structure of cations in aqueous salt solutions was also investigated by the O K-edge XAS.[53,54] Wilson et al. studied the O and C K-edge XAS of liquid methanol in the total electron yield of liquid microjet.[55] Tamenori et al. measured the O and C K-edge XAS of free methanol clusters.[56] Guo et al. investigated liquid methanol and methanol−water binary solutions at X = 0.5 by using the O K-edge XAS and X-ray emission spectroscopy.[57,58] Guo et al. suggested that liquid methanol shows chains and rings of 6−8 methanol molecules and proposed that the number of pure methanol chains decreases and the number of mixed methanol−water networks increases when adding water molecules. However, the O K-edge XAS shows contributions of oxygen atoms in both methanol and water molecules and is difficult to analyze the local structure of methanol−water mixtures. It is necessary to measure the C K-edge XAS to analyze the local structure of the methyl group of methanol molecules in the binary solution.

In the present work, we investigate the local structure of methanol−water binary solutions at different concentrations by the O and C K-edge XAS. The XAS measurement is based on a transmission mode by using a recently developed liquid cell that enables to optimize the absorbance by changing the thickness of liquid layer.[59] The pre-edge feature in the O K-edge XAS is found to show almost linear dependence of the concentration. On the other hand, in the C K-edge XAS, the second peak that is related to the methyl group is found to change its behavior at X = 0.7 and X = 0.3. With the help of the MD simulation, we have revealed different local structures of methanol−water mixtures at the three concentration regions.

2. EXPERIMENTS

The experiments were performed at an in-vacuum soft X-ray undulator beamline BL3U at UVSOR-II.[60] Details of the liquid cell were described previously.[59,61] The liquid cell consists of four regions, which are separated by 100 nm thick Si_3N_4 membranes (NTT AT Co., Ltd.). Soft X-rays under vacuum (region I) pass through the buffer region filled with helium gas (region II) and the liquid thin layer (region III) and finally reach a photodiode detector filled with helium gas (region IV). The regions II and IV are connected and can be mixed with other gas molecules for the precise gas−liquid energy shift measurement and photon energy calibration. A liquid sample (region III) is sandwiched between two Si_3N_4 membranes with pressed Teflon spacers and can be substituted by other samples in combination with a tubing pump system.

The thickness of liquid layer should be optimized in order to transmit soft X-rays with an appropriate absorbance.[62] In the present liquid cell, the thickness of the liquid layer can be controlled from 2000 to 20 nm by increasing the helium pressure in the regions II and IV. The thickness is set to 300 nm in the present O K-edge XAS. In the C K-edge XAS, on the other hand, the thickness of liquid methanol is set to 550 nm, and the thickness is set larger in more dilute methanol aqueous solutions. The energy resolutions of incident soft X-rays at the O and C K-edges are set to 0.40 and 0.19 eV, respectively. The XAS spectra are based on the Beer−Lambert law, $\ln(I_0/I)$, where I_0 and I are the detection current through the cell without and with samples, respectively. The liquid flow is stopped during the XAS measurement because the sample liquid has no radiation damage from the long (say, more than 1 h) exposure of soft X-rays in the present photon flux. The photon energy in the O K-edge is calibrated by the O 1s π^* peak (530.80 eV)[63] for free O_2 molecules and that in the C K-edge is calibrated by the first peak (287.96 eV)[56] of free methanol molecules, which are mixed with helium gas in the regions II and IV.

3. RESULTS AND DISCUSSION

3.1. Oxygen K-Edge XAS. Figure 1 shows O K-edge XAS spectra for methanol−water binary solutions at different concentrations at 25 °C. The absorbance in the O K-edge XAS spectra was normalized by the sample thickness and the concentration of the binary solution considering the soft X-ray absorption coefficients of water and methanol in the O K-edge.[62] After this normalization, we subtracted a constant background and show the resultant absorption coefficients in Figure 1. In the previous work,[57] a small peak was observed around 532 eV in methanol−water mixtures; on the other hand, it is not observed for any concentration in the present measurement. It should not be regarded as an intrinsic peak. The pre-edge peak of liquid water (534.7 eV) corresponds to the O 1s transition to an unoccupied $4a_1$* orbital of a water molecule (533.9 eV), which is mainly distributed at the oxygen atom in water molecule and is blue-shifted and broadened by the HB interaction.[51] On the other hand, the pre-edge feature of liquid methanol (534.9 eV) is embedded in the main peak but is similarly blue-shifted from the gas-phase peak (534.0 eV).[55]

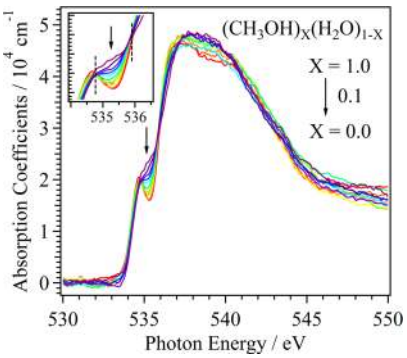

Figure 1. O K-edge XAS spectra of methanol−water binary solutions at different concentrations at 25 °C. The mixing ratio of methanol in the solution decreases with molar fraction steps of 0.1 along indicated arrows. The inset shows isosbestic points (dashed lines) in the pre-edge region.

Figure 1 shows that the intensity of the pre-edge region around 535.2 eV decreases as the molar fraction of methanol

dx.doi.org/10.1021/jp4091602 | J. Phys. Chem. B 2014, 118, 4388−4396

(X) decreases in the binary solution $(CH_3OH)_X(H_2O)_{1-X}$. It is known that the pre-edge peak in liquid water reflects the HB interaction, and the intensity of methanol is different from that of water. The pre-edge region shows isosbestic points at 534.8 and 535.9 eV. It indicates that the pre-edge region in the XAS spectrum contains only two contributions, which is the HB interaction of liquid methanol and that of liquid water. In order to obtain the change in the HB interaction at the different concentrations, the pre-edge region between 534 and 536 eV in the O K-edge XAS spectra at the different concentrations is fitted by the superposition of pure liquid methanol (X = 1.0) and pure liquid water (X = 0.0), as shown in Figure 2.

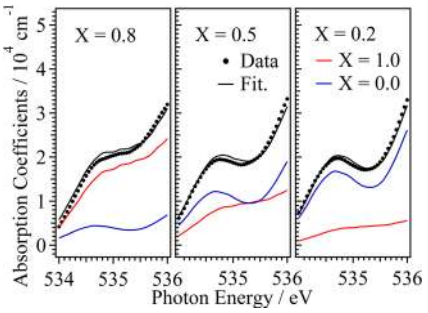

Figure 2. Fitting results of the pre-edge region in the O K-edge XAS spectra at the molar fractions of X = 0.8, X = 0.5, and X = 0.2 in the methanol−water binary solutions $(CH_3OH)_X(H_2O)_{1-X}$ by superposition of the reference spectra of pure liquid methanol (X = 1.0) and pure liquid water (X = 0.0).

Figure 3 shows the fraction of the pure methanol contribution in the pre-edge region as a molar fraction step

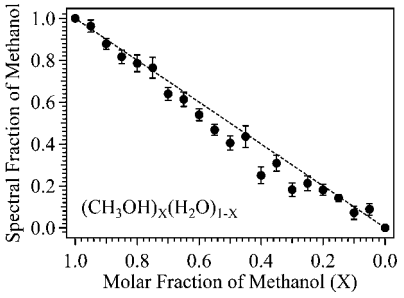

Figure 3. Fraction of the pure methanol contribution in the pre-edge region of the O K-edge XAS spectra as a function of the methanol molar fraction (X) in the methanol−water binary solutions $(CH_3OH)_X(H_2O)_{1-X}$, which is obtained by fitting from superposition of pure liquid methanol (X = 1.0) and pure liquid water (X = 0.0). Each fraction includes an error bar.

of 0.05, which corresponds to the HB interaction. The intensity decreases almost linearly as the molar fraction of methanol decreases. There may be some information about different local structures on the oxygen atom behind small deviations from the linear dependence, but it is consistent with the result of vibrational spectroscopy,[22,24] which explains that the ratio of HB interaction of methanol−methanol to that of methanol−water is linearly dependent on the molar fraction of methanol.

Observation of the isosbestic points suggests that the binary solution has two major HB components, though there are four different HB interactions: O_m*HO_m, O_m*HO_w, O_w*HO_m, and O_w*HO_w, where O_m and O_w denote oxygen atoms of methanol and water, respectively, and the asterisk denotes the atom with an O 1s hole. There are two possibilities. One is a negligible HB interaction between water and methanol, O_m*HO_w and O_w*HO_m, indicating that water aggregates are segregated from methanol ones in solution. The other is almost the same HB interaction in O_w*HO_m as in O_w*HO_w and that in O_m*HO_w as in O_m*HO_m. The pre-edge peak of liquid water is sensitive to the HB interaction of liquid water and is dependent on the temperature.[52] The concentration dependence in the pre-edge region of the methanol−water binary solution is smaller than the temperature dependence of liquid water. Therefore, nearly the same HB interaction between methanol and water could be possible.

3.2. Carbon K-Edge XAS. Figure 4 shows C K-edge XAS spectra of molecular (gas) and liquid methanol at 25 °C by

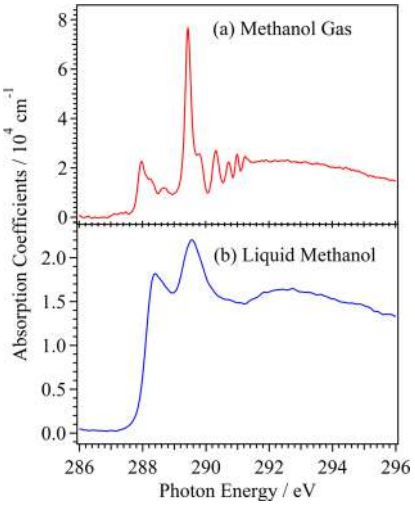

Figure 4. C K-edge XAS spectra of (a) methanol gas and (b) liquid methanol at 25 °C.

using the same sample cell. The XAS spectrum of methanol gas was measured by mixing methanol vapor into helium buffer gas and is in agreement with published spectra.[55,56,64,65] As shown in Figure 4a, the first peak (287.96 eV) in a gas-phase spectrum arises from a transition of the C 1s electron to the lowest unoccupied orbital (8a′) of C−O antibonding and O−H bonding characters. The second peak around 289.44 eV arises from a transition of the C 1s electron to the second lowest unoccupied orbital (9a′) of pseudo CH_3-π* character with a very small OH component. The broad peak around 293 eV arises from a transition of the C 1s electron to the highest unoccupied orbital (11a′) within a minimal basis picture, which is of both C−O antibonding and O−H antibonding character.

Figure 4b shows the present C K-edge XAS spectrum of liquid methanol with a simple structure of three main contributions around 288.4, 289.55, and 293 eV. The published C K-edge XAS spectrum of free methanol clusters[56] is almost the same as the present liquid spectrum. On the other hand, the published spectrum of liquid microjet methanol[55] is different from the present one and is rather similar to the gas-phase spectrum. It could be difficult to completely remove the contribution from the molecular methanol in the liquid microjet experiment.

In the liquid spectrum, the first peak (8a′-related), which is an excited state with both CH_3 and OH components, shows a 0.44 eV blue-shift from that in the gas spectrum. On the other hand, the second peak (9a′-related), which is an excited state

dx.doi.org/10.1021/jp4091602 | J. Phys. Chem. B 2014, 118, 4388−4396

with a large CH_3 component, shows a 0.11 eV blue-shift from that in the gas spectrum. Considering atomic components in the corresponding molecular orbitals of a methanol molecule, the second excited state has mainly a hydrophobic interaction, but the first excited state has not only a hydrophobic interaction but also an HB interaction. The unoccupied orbital level could be destabilized by both the hydrophobic and hydrophilic interactions in liquid, similarly to the case of the blue-shifted O 1s pre-edge peak in liquid water as observed in Figure 1.

Figure 5 shows C K-edge XAS spectra of methanol−water binary solutions of different concentrations at 25 °C. The C K-edge XAS spectrum is more appropriate than the O K-edge XAS as regards the analysis of the intermolecular interaction of methanol because the carbon atom is contained only in methanol. The absorbance in the C K-edge XAS spectra was normalized by the sample thickness and the concentration of the binary solution considering the soft X-ray absorption coefficients of methanol in the C K-edge.[62] After this normalization, we subtracted the absorbance of water in the C K-edge by considering the sample thickness, the concentration of the binary solution, and the soft X-ray absorption coefficient of water in the C K-edge.[62] Figure 5 shows resultant absorption coefficients. The first peak that is related to the HB interaction of the OH and CH_3 groups does not change its energy position so much at different concentrations. This is reasonable if the HB interaction of methanol with water is not so different from that with methanol and is consistent with the results of O K-edge XAS shown in Figure 3.

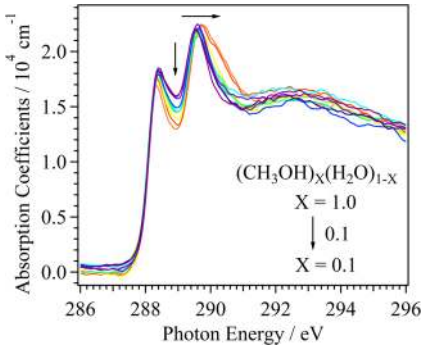

Figure 5. C K-edge XAS spectra of methanol−water binary solutions at different concentrations at 25 °C. The mixing ratio of methanol in the solution decreases with molar fraction steps of 0.1 along indicated arrows.

On the other hand, the second peak, which corresponds to the excited state with a large CH_3 component, increases the blue-shift as the mixing ratio of water increases. It is reasonable, considering that the blue-shift arises from the interaction of methyl group in methanol molecule. Liquid methanol forms 1D/2D network structures, and the methyl groups are apart from each other due to its hydrophobic interaction. When water molecules join the 1D/2D HB network of methanol, the 3D HB network might be formed. Then, the interaction of methyl groups can be enhanced in binary solutions and causes the blue-shift of the second peak in the C K-edge XAS spectra. The general behavior observed in Figure 5 is consistent with that of the neutron diffraction,[11] where mixed methanol−water networks are formed and methyl groups become closer to each other in the methanol−water binary solution.

Because the second peak related to the methyl group shows a quasi-isosbestic point around 290 eV, two contributions would be contained in the second peak: One is the interaction of surrounding methanol with the methyl group, which is obtained by the C K-edge XAS spectrum of liquid methanol (X = 1.0). The other is the hydrophobic interaction of surrounding water with the methyl group, which is obtained by the XAS spectrum of the dilute methanol solutions (X = 0.05). In order to obtain the change in the hydrophobic interaction of methyl group at the different concentrations, the second peak between 288.5 and 290.5 eV in the C K-edge XAS spectra at the different concentrations are fitted by superposition of the reference spectra of liquid methanol (X = 1.0) and the dilute methanol solution (X = 0.05), as shown in Figure 6.

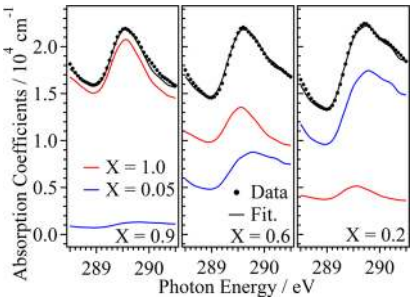

Figure 6. Fitting results of the second peak in the C K-edge XAS spectra at the molar fractions of X = 0.9, X = 0.6, and X = 0.2 in the methanol−water binary solutions $(CH_3OH)_X(H_2O)_{1-X}$ by superposition of the reference spectra of pure liquid methanol (X = 1.0) and the dilute methanol solution (X = 0.05).

Figure 7 shows the fraction of the pure liquid methanol contribution in the second peak at different molar fractions of methanol (X) in the binary solution $(CH_3OH)_X(H_2O)_{1-X}$, which corresponds to the hydrophobic interaction of the methyl group. The fraction of the pure liquid methanol contribution is changed nonlinearly and shows three different behaviors with the borders of X = 0.7 and X = 0.3. In the methanol-rich region I (X > 0.7), the intensity is not so much changed as compared to the intensity of liquid methanol (X = 1.0). The phase transition-like behavior of the intensity change is found at X = 0.7. The slow decrease in intensity (indicating blue-shift of the second pre-edge peak) continues when

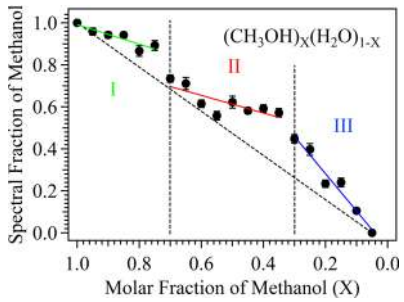

Figure 7. Fraction of the pure liquid methanol contribution in the second peak in the C K-edge XAS spectra as a function of the methanol molar fraction (X) in the methanol−water binary solutions $(CH_3OH)_X(H_2O)_{1-X}$, which is obtained by fitting from superposition of pure liquid methanol (X = 1.0) and the dilute methanol solution (X = 0.05). Each fraction includes an error bar. Three characteristic regions are found with the borders of X = 0.7 and X = 0.3.

dx.doi.org/10.1021/jp4091602 | J. Phys. Chem. B 2014, 118, 4388−4396

increasing the mixing ratio of water in the region II ($0.7 > X > 0.3$). The decrease in intensity becomes faster in the water-rich region III ($0.30 > X > 0.05$). These results suggest different local interactions of the methyl group at the different concentration regions.

3.3. MD Simulations. Without any spectral calculation based on time-consuming density functional theory or ab initio approaches, it would be simply understood that the C K-edge region is sensitive to the hydrophobic interaction around the methyl group of methanol. In order to get such information from the radial distribution function (RDF) of intermolecular interaction in the solutions, we have carried out the MD simulation by using GROMACS 4.5.5.[66] The potential of methanol molecule is described by OPLSAA,[67,68] and that of water molecule is TIP5P.[69] The temperature is controlled by the Nosé–Hoover thermostat method.[70] The pressure is adjusted by the Parrinello–Rahman method.[71] The simulation was performed at a time step of 1 fs with a periodic boundary condition and the particle-mesh Ewald method.[72] The unit cell consists of 500 molecules, and the molar fraction of methanol (X) is changed from $X = 0.0$ to $X = 1.0$. Randomly distributed structures were optimized by the simulations, which run during 50 ps at 100 K in the NVT condition, 50 ps at 200 K and 1 atm in the NPT condition, and 400 ps at 298.15 K and 1 atm in the NPT condition. The equilibrium structures were obtained by sampling the structures every 1 ps during a simulation time of 2 ns.

First, we calculated RDF of four different HB: O_m–HO_m, O_m–HO_w, O_w–HO_m, and O_w–HO_w. The distances of both the first peak and the first minimum point in RDF are not changed even at different molar fractions. It means that the HB interaction of water is nearly the same as that of methanol as already discussed in the O K-edge XAS.

The number of HB was counted at different molar fractions, based on the criterion of the distance between HO and O within the first minimum point (2.5 Å) in RDF.[73] By increasing the molar fraction of water, the total number of HB increases linearly. The average number of HB around water molecules is between 3.2 and 3.8, and that around methanol is between 1.8 and 2.5. This is consistent, considering the water molecule has two donor and two acceptor sites and the methanol molecule has one donor and one or two acceptor sites. The total average number of HB is increasing at the higher mixing ratio of water molecules.

Figure 8 shows RDF of C in the methyl group of methanol with surrounding atoms at different molar fractions of methanol (X) in the binary solution $(CH_3OH)_X(H_2O)_{1-X}$. Figure 8a shows RDF of C with C and hydrogen H (HC) atoms in the CH_3 group of neighboring methanol molecules. The RDF distances of both C–C and C–HC are slightly reduced by increasing the mixing ratio of water. This result is consistent with the results of neutron diffraction.[11] Figure 8b shows RDF of C with O_m and HO_m in neighboring methanol molecules. The intensities of both HO_m and O_m in the first coordination peak decrease as increasing the mixing ratio of water. On the other hand, as shown in Figure 8c, the intensities of both HO_w and O_w in the first coordination peak increase as increasing the mixing ratio of water.

Figure 9 shows the number of the coordination by nearest neighbors HO_m and HO_w to the C atom in the methyl group of methanol at different binary solutions. The coordination is defined within the RDF distance of 3.2 Å, which is the first minimum point of HO_m and HO_w as shown in Figure 8. The

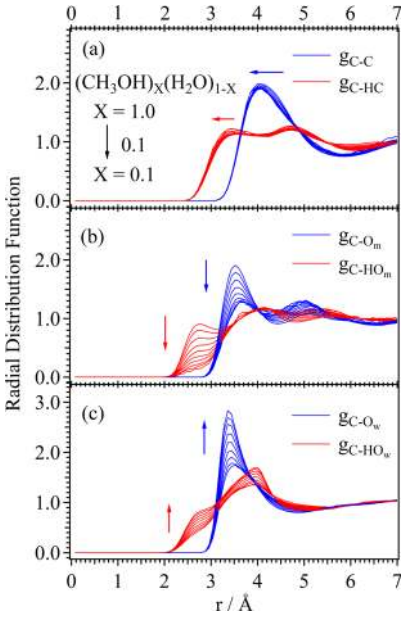

Figure 8. Results of the MD simulation for the RDF of the C atom with surrounding atoms: (a) C and HC in methanol, (b) O_m and HO_m in methanol, and (c) O_w and HO_w in water. The mixing ratio of methanol in the solution decreases from $X = 1.0$ to $X = 0.1$ with molar fraction steps of 0.1 along indicated arrows. Note that RDF in (c) is changed from $X = 0.9$ to $X = 0.1$.

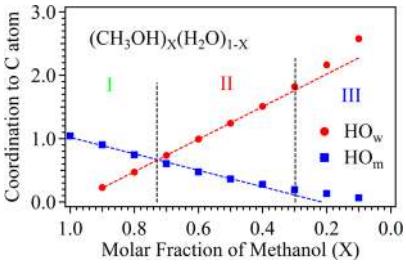

Figure 9. Results of the MD simulation for the coordination numbers of HO_m (square) and HO_w (circle) to the C atom of the methyl group of methanol at different molar fractions of methanol (X) in the binary solutions $(CH_3OH)_X(H_2O)_{1-X}$. Below $X = 0.73$ (region II), the coordination number of HO_w becomes larger than that of HO_m. In the region III ($0.3 > X$), the linear dependence of HO_m and HO_w is not valid as shown by dashed lines.

methyl group in liquid methanol ($X = 1.0$) is surrounded by HO_m (square). By increasing the molar fraction of water, the number of HO_m coordination decreases and instead that of HO_w (circle) increases. When the methanol molar fraction is below $X = 0.7$, the number of HO_w coordination becomes larger than the HO_m coordination. It is reasonable considering that the molar ratio of methanol and water is 2:1 at $X = 0.67$ and the ratio of the H donating site is 1:1. However, the rate of increase in the number of HO_w coordination is larger than the rate of decrease in the number of HO_m coordination. The rate of increase in the number of HO_w coordination is accelerated in the region III ($0.3 > X$). On the other hand, the number of HO_m coordination is nearly zero in the region III. Note that $X = 0.7$ and $X = 0.3$ are almost the same borders in the spectral change of the C K-edge XAS as shown in Figure 7.

Next, we investigate the mesoscopic scale HB network in the binary solution. The average size of methanol clusters in pure liquid methanol ($X = 1.0$) is 40 in the present MD simulation,

dx.doi.org/10.1021/jp4091602 | J. Phys. Chem. B 2014, 118, 4388–4396

which contains 500 molecules. The hydrophobic interaction of the methyl group prevents a large HB network formation and permits only formation of small methanol clusters with an average size of 40. This size is larger than the previously predicted size, 6−8 molecules.[8]

On the other hand, water molecules like to meet (bond) together to form a large HB network in solution. Figure 10

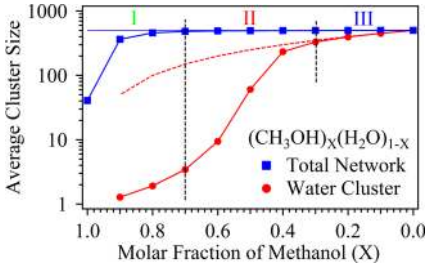

Figure 10. Results of the MD simulation for the average HB network size (square) and the average size of water-only clusters (circle) embedded in total HB networks in a unit cell (500 molecules) of the binary solution $(CH_3OH)_X(H_2O)_{1-X}$ as a function of molar fraction of methanol (X). The dashed line is a total number of water molecules in the solution.

shows results of the MD simulation for the average HB network size and the average size of water-only clusters embedded in total HB networks at different molar fractions of methanol (X) in the binary solutions $(CH_3OH)_X(H_2O)_{1-X}$. A unit cell in the present MD simulation contains totally 500 molecules.

In the methanol-rich region I ($X > 0.7$), the average size of water-only clusters is rather small considering that a water molecule is difficult to meet another water molecule in this region. Water clusters start to grow at $X = 0.7$. As the molar fraction of methanol is down to $X = 0.3$ in the region II ($0.7 > X > 0.3$), the rate of growing in size of water clusters is accelerated, and finally the average size of water clusters is equal to the total number of water molecules in the region III. On the other hand, at $X = 0.7$, all the methanol and water molecules join a large HB network, though a large water-only cluster is not yet formed in the network. The ratio of the total number of H donating (accepting) sites is 1:1 for water and methanol at $X = 0.67$; therefore, all the water and methanol molecules can meet (bond) together to form a large HB network at around $X = 0.7$.

3.4. Structures of Methanol−Water Mixtures. From the result of the C K-edge XAS shown in Figure 7, the interaction around the methyl group of methanol molecule shows characteristic changes at the three concentration regions. The MD simulations also show similar three concentration regions from the coordination number around the methyl group shown in Figure 9 and the average cluster size shown in Figure 10.

Figure 11a shows a typical structure in the binary solution at $X = 0.9$ in the methanol-rich region I. As shown in Figure 10, the average size of water-only clusters is much smaller than the total number of water molecules. Water molecules form the HB network with methanol clusters and stabilize the total energy of the binary solution. However, the interaction around the methyl group of methanol is not so much influenced by water molecules because of a small amount of isolated water molecules. It is consistent with the previous work,[16,27] where water molecules are coordinated to the terminal of methanol chains in the methanol-rich region.

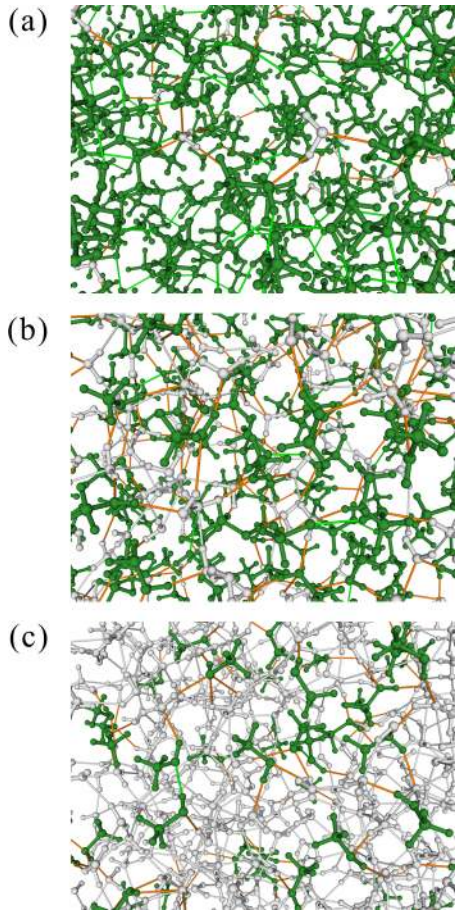

Figure 11. Typical structures of methanol−water binary solutions at different concentrations: (a) $X = 0.9$, (b) $X = 0.5$, and (c) $X = 0.1$. Methanol and water molecules are marked as green and white, respectively. HB between methanol and water is marked as an orange line.

Figure 7 shows a phase-transition-like intensity change at $X = 0.7$ in the C K-edge XAS. Figure 9 shows that the number of HO_w coordination to the methyl group becomes larger than that of HO_m coordination below $X = 0.7$. In addition, Figure 10 shows that the HB network of water clusters grows rapidly below $X = 0.7$. Figure 11b shows a typical structure in the binary solution at $X = 0.5$ in the region II. Water molecules form a large cluster and have the 3D HB network with methanol molecules, resulting in the increase of the interaction of the methyl group in methanol with water molecules. The phase-transition-like behavior at $X = 0.7$ in the C K-edge XAS (Figure 7) indicates that the 3D HB network involving water clusters is dominant over the 1D/2D HB network of methanol in the binary solutions. This result is consistent with the previous MD simulation, in which the 1D chain structure of methanol molecules is changed to 3D mixed clusters by adding water molecules.[40]

Figure 11c shows a typical structure in the binary solution at $X = 0.1$ in the water-rich region III. The HB networks between methanol molecules are mostly diminished, and methanol molecules are isolated in the 3D HB network of water. The hydration structures of methanol molecules are dominated by the 3D HB network of water, and the numbers of water coordination to the methyl group increase. As a result, the hydrophobic interaction around the methyl group is enhanced in this region, increasing a blue-shift in the C K-edge XAS. The

dx.doi.org/10.1021/jp4091602 | J. Phys. Chem. B 2014, 118, 4388−4396

previous theoretical studies suggested that hydration structures of methanol molecules are formed in this concentration region,[41,43,45] consistent with the present result.

It is known that the thermodynamic parameter such as entropy and viscosity shows an extreme value at the molar fraction of $X = 0.30$.[1,2] Dougan et al. studied neutron diffraction experiments and MD simulations and suggested that both methanol and water molecules are percolated in this region, and the thermodynamic parameters show extreme values at the molar fraction of $X = 0.27$.[12] It means that the structure and abundance of large mixed methanol−water HB networks in the binary solution, as clearly shown in Figures 9 and 10, affect macroscopic thermodynamic properties.

4. CONCLUSIONS

The local structure of methanol−water binary solutions was studied by the O and C K-edge XAS. The pre-edge peak in the O K-edge XAS reflects the HB interaction of oxygen atoms and shows almost linear concentration dependence. It indicates that the HB interaction of methanol with surrounding water molecules is nearly the same as in pure liquid methanol and the HB interaction of water with surrounding methanol molecules is nearly the same as in pure liquid water.

The C K-edge XAS enables us exclusively to investigate local structures around the methyl group of methanol molecules in the binary solution. The peak around 290 eV in the C K-edge XAS corresponds to a transition of the C 1s electron to the unoccupied orbital around the methyl group and shows the higher photon energy (blue-shift) as the mixing ratio of water increases. It predicts enhancement in the interaction between the hydrophobic methyl groups by large water clusters in mixed methanol−water networks. The intensity change shows a nonlinear profile with three characteristic concentration regions in the binary solution $(CH_3OH)_X(H_2O)_{1-X}$.

The three regions are consistently interpreted with the help of the MD simulation. Liquid methanol is known to have the 1D/2D HB network structure.[8] In the methanol-rich region I ($X > 0.7$), a small amount of water molecules form the HB network with methanol clusters and stabilize the total energy of the binary solution. However, the interaction around the methyl group of methanol is not so much influenced by isolated water molecules. The phase-transition-like decrease in the intensity occurs at the molar fraction of $X = 0.7$. The 3D HB network of water start to grow rapidly, and the HO_w coordination to the methyl group becomes dominant over the HO_m coordination when the molar fraction is below $X = 0.7$. In the region II ($0.7 > X > 0.3$), methanol molecules form a large HB network with water molecules. As a result, the hydrophobic interaction of the methyl group is enhanced in this region. This behavior is reasonable considering that the molar ratio of methanol and water is 2:1 at $X = 0.67$ and the ratio of the H donating site is 1:1. The thermodynamic parameters such as entropy and viscosity are closer to extreme values as the number of mixed HB networks increases at $X = 0.3$. In the water-rich region III ($0.3 > X > 0.05$), the interaction of surrounding water molecules with the methyl group is increased rapidly, indicating methanol molecules are separately embedded in the 3D HB network of water molecules.

The methyl group in the methanol−water binary solution shows three characteristic local structures: methanol-dominant 1D/2D HB network structure with isolated water molecules, methanol−water mixed 3D HB network structure, and water-dominant 3D HB network structure with isolated methanol molecules. These features are successfully revealed by the fitting analysis of the second peak in the C K-edge XAS, which is sensitive to the hydrophobic interaction of the methyl group, and the MD simulation.

AUTHOR INFORMATION

Corresponding Author

*E-mail: kosugi@ims.ac.jp (N.K.).

Present Address

V.L.: École Nationale Supérieure de Chimie de Paris (Chimie ParisTech), Paris, 75231 Cedex 05, France.

Notes

The authors declare no competing financial interest.

ACKNOWLEDGMENTS

This work is supported by JSPS Grants-in-Aid for Scientific Research (Nos. 20350014, 23245007, and 23685006). The authors acknowledge Dr. Takaki Hatsui and Mr. Toshio Horigome for the contributions of the liquid cell and the staff members of the UVSOR-II facility for their kind support. Theoretical calculations were performed at Research Center for Computational Science, Okazaki, Japan.

REFERENCES

(1) Frank, H. S.; Evans, M. W. Free volume and entropy in condensed systems. III. Entropy in binary liquid mixtures; Partial molal entropy in dilute solutions; structure and thermodynamics in aqueous electrolytes. *J. Chem. Phys.* **1945**, *13*, 507−532.

(2) Mikhail, S. Z.; Kimel, W. R. Densities and viscosities of methanol-water mixtures. *J. Chem. Eng. Data* **1961**, *6*, 533−537.

(3) Ludwig, R. Water: From clusters to the bulk. *Angew. Chem., Int. Ed.* **2001**, *40*, 1808−1827.

(4) Magini, M.; Paschina, G.; Piccaluga, G. On the structure of methyl alcohol at room temperature. *J. Chem. Phys.* **1982**, *77*, 2051−2056.

(5) Narten, A. H.; Habenschuss, A. Hydrogen bonding in liquid methanol and ethanol determined by x-ray diffraction. *J. Chem. Phys.* **1984**, *80*, 3387−3391.

(6) Tanaka, Y.; Ohtomo, N.; Arakawa, K. The structure of liquid alcohols by neutron diffraction. I. Molecular structure of methyl alcohol. *Bull. Chem. Soc. Jpn.* **1984**, *57*, 644−647.

(7) Tanaka, Y.; Ohtomo, N.; Arakawa, K. The structure of liquid alcohols by neutron and X-ray diffraction. III. Liquid structure of methanol. *Bull. Chem. Soc. Jpn.* **1985**, *58*, 270−276.

(8) Sarkar, S.; Joarder, R. N. Molecular clusters and correlations in liquid methanol at room temperature. *J. Chem. Phys.* **1993**, *99*, 2032−2039.

(9) Yamaguchi, T.; Hidaka, K.; Soper, A. K. The structure of liquid methanol revisited: a neutron diffraction experiment at −80 °C and +25 °C. *Mol. Phys.* **1999**, *96*, 1159−1168.

(10) Soper, A. K.; Finney, J. L. Hydration of methanol in aqueous solution. *Phys. Rev. Lett.* **1993**, *71*, 4346−4349.

(11) Dixit, S.; Crain, J.; Poon, W. C. K.; Finney, J. L.; Soper, A. K. Molecular segregation observed in a concentrated alcohol-water solution. *Nature* **2002**, *416*, 829−832.

(12) Dougan, L.; Bates, S. P.; Hargreaves, R.; Fox, J. P.; Crain, J.; Finney, J. L.; Réat, V.; Soper, A. K. Methanol-water solutions: A bi-percolating liquid mixture. *J. Chem. Phys.* **2004**, *121*, 6456−6462.

(13) Corsaro, C.; Spooren, J.; Branca, C.; Leone, N.; Broccio, M.; Kim, C.; Chen, S.; Stanley, H. E.; Mallamace, F. Clustering dynamics in water/methanol mixtures: A nuclear magnetic resonance study at 205 K < T < 295 K. *J. Phys. Chem. B* **2008**, *112*, 10449−10454.

(14) Takamuku, T.; Yamaguchi, T.; Asato, M.; Matsumoto, M.; Nishi, N. Structure of clusters in methanol-water binary solutions studied by mass spectrometry and X-ray diffraction. *Z. Naturforsch.* **2000**, *55*, 513−525.

(15) Micali, N.; Trusso, S.; Vasi, C.; Blaudez, D.; Mallamace, F. Dynamical properties of water-methanol solutions studied by depolarized Rayleigh scattering. *Phys. Rev. E* **1996**, *54*, 1720−1724.
(16) Sato, T.; Chiba, A.; Nozaki, R. Hydrophobic hydration and molecular association in methanol-water mixtures studied by microwave dielectric analysis. *J. Chem. Phys.* **2000**, *112*, 2924−2932.
(17) Falk, M.; Whalley, E. Infrared spectra of methanol and deuterated methanols in gas, liquid, and solid phases. *J. Chem. Phys.* **1961**, *34*, 1554−1568.
(18) Passchier, W. F.; Klompmaker, E. R.; Mandel, M. Absorption spectra of liquid and solid methanol from 1000 to 100 cm^{-1}. *Chem. Phys. Lett.* **1970**, *4*, 485−488.
(19) Bertie, J. E.; Zhang, S. L.; Eysel, H. H.; Baluja, S.; Ahmed, M. K. Infrared intensities of liquids XI: Infrared refractive indices from 8000 to 2 cm^{-1}, absolute integrated intensities, and dipole moment derivatives of methanol at 25 °C. *Appl. Spectrosc.* **1993**, *47*, 1100−1114.
(20) Venables, D. S.; Schmuttenmaer, C. A. Spectroscopy and dynamics of mixtures of water with acetone, acetonitrile, and methanol. *J. Chem. Phys.* **2000**, *113*, 11222−11236.
(21) Adachi, D.; Katsumoto, Y.; Sato, H.; Ozaki, Y. Near-infrared spectroscopic study of interaction between methyl group and water in water-methanol mixtures. *Appl. Spectrosc.* **2002**, *56*, 357−361.
(22) Ma, G.; Allen, H. C. Surface studies of aqueous methanol solutions by vibrational broad bandwidth sum frequency generation spectroscopy. *J. Phys. Chem. B* **2003**, *107*, 6343−6349.
(23) Woods, K. N.; Wiedemann, H. The influence of chain dynamics on the far-infrared spectrum of liquid methanol-water mixtures. *J. Chem. Phys.* **2005**, *123*, 134507.
(24) Ahmed, M. K.; Ali, S.; Wojcik, E. The C-O stretching infrared band as a probe of hydrogen bonding in ethanol-water and methanol-water mixtures. *Spectrosc. Lett.* **2012**, *45*, 420−423.
(25) Kabisch, G.; Pollmer, K. Hydrogen bonding in methanol-organic solvent and methanol-water mixtures as studied by the ν_{CO} and ν_{OH} Raman Bands. *J. Mol. Struct.* **1982**, *81*, 35−50.
(26) Schwartz, M.; Moradi-Araghi, A.; Koehler, W. H. Solvent and temperature dependence of the Fermi resonance parameters in methanol. *J. Mol. Struct.* **1982**, *81*, 245−252.
(27) Dixit, S.; Poon, W. C. K.; Crain, J. Hydration of methanol in aqueous solutions: a Raman spectroscopic study. *J. Phys.: Condens. Matter* **2000**, *12*, L323−L328.
(28) Lin, K.; Zhou, X.; Luo, Y.; Liu, S. The microscopic structure of liquid methanol from Raman spectroscopy. *J. Phys. Chem. B* **2010**, *114*, 3567−3573.
(29) Haughney, M.; Ferrario, M.; McDonald, I. R. Molecular-dynamics simulation of liquid methanol. *J. Phys. Chem.* **1987**, *91*, 4934−4940.
(30) Ferrario, M.; Haughney, M.; McDonald, I. R.; Klein, M. L. Molecular-dynamics simulation of aqueous mixtures: Methanol, acetone, and ammonia. *J. Chem. Phys.* **1990**, *93*, 5156−5166.
(31) Skaf, M. S.; Ladanyi, B. M. Molecular dynamics simulation of solvation dynamics in methanol-water mixtures. *J. Phys. Chem.* **1996**, *100*, 18258−18268.
(32) Laaksonen, A.; Kusalik, P. G.; Svishchev, I. M. Three-dimensional structure in water-methanol mixtures. *J. Phys. Chem. A* **1997**, *101*, 5910−5918.
(33) Tsuchida, E.; Kanada, Y.; Tsukada, M. Density-functional study of liquid methanol. *Chem. Phys. Lett.* **1999**, *311*, 236−240.
(34) van Erp, T. S.; Meijer, E. J. Hydration of methanol in water. A DFT-based molecular dynamics study. *Chem. Phys. Lett.* **2001**, *333*, 290−296.
(35) Morrone, J. A.; Tuckerman, M. E. Ab initio molecular dynamics study of proton mobility in liquid methanol. *J. Chem. Phys.* **2002**, *117*, 4403−4412.
(36) Pagliai, M.; Cardini, G.; Righini, R.; Schettino, V. Hydrogen bond dynamics in liquid methanol. *J. Chem. Phys.* **2003**, *119*, 6655−6662.
(37) Handgraaf, J.-W.; Meijer, E. J.; Gaigeot, M.-P. Density-functional theory-based molecular simulation study of liquid methanol. *J. Chem. Phys.* **2004**, *121*, 10111−10119.
(38) Yu, H.; Geerke, D. P.; Liu, H.; Van Gunsteren, W. F. Molecular dynamics simulations of liquid methanol and methanol-water mixtures with polarizable models. *J. Comput. Chem.* **2006**, *27*, 1494−1504.
(39) Zhong, Y.; Warren, G. L.; Patel, S. Thermodynamic and structural properties of methanol-water solutions using nonadditive interaction models. *J. Comput. Chem.* **2007**, *29*, 1142−1152.
(40) Bakó, I.; Megyes, T.; Bálint, S.; Grósz, T.; Chihaia, V. Water-methanol mixtures: topology of hydrogen bonded network. *Phys. Chem. Chem. Phys.* **2008**, *10*, 5004−5011.
(41) Silvestrelli, P. L. Are there immobilized water molecules around hydrophobic groups? Aqueous solvation of methanol from first principles. *J. Phys. Chem. B* **2009**, *113*, 10728−10731.
(42) Ishiyama, T.; Sokolov, V. V.; Morita, A. Molecular dynamics simulation of liquid methanol. I. Molecular modeling including C-H vibration and fermi resonance. *J. Chem. Phys.* **2011**, *134*, 024509.
(43) Moin, S. T.; Hofer, T. S.; Randolf, B. R.; Rode, B. M. Structure and dynamics of methanol in water: A quantum mechanical charge field molecular dynamics Study. *J. Comput. Chem.* **2011**, *32*, 886−892.
(44) Jorgensen, W. L. Structure and properties of liquid methanol. *J. Am. Chem. Soc.* **1980**, *102*, 543−549.
(45) Okazaki, S.; Touhara, H.; Nakanishi, K. Computer experiments of aqueous solutions. V. Monte Carlo calculation on the hydrophobic interaction in 5 mol% methanol solution. *J. Chem. Phys.* **1984**, *81*, 890−894.
(46) Adamovic, I.; Gordon, M. S. Methanol-water mixtures: A microsolvation study using the effective fragment potential method. *J. Phys. Chem. A* **2006**, *110*, 10267−10273.
(47) Valdéz-González, M.; Saint-Martin, H.; Hernández-Cobos, J. Liquid methanol Monte Carlo simulations with a refined potential which includes polarizability, nonadditivity, and intramolecular relaxation. *J. Chem. Phys.* **2007**, *127*, 224507.
(48) da Silva, J. A. B.; Moreira, F. G. B.; dos Santos, V. M. L.; Longo, R. L. On the hydrogen bond networks in the water-methanol mixtures: topology, percolation and small-world. *Phys. Chem. Chem. Phys.* **2011**, *13*, 6452−6461.
(49) da Silva, J. A. B.; Moreira, F. G. B.; dos Santos, V. M. L.; Longo, R. L. Hydrogen bond networks in water and methanol with varying interaction strengths. *Phys. Chem. Chem. Phys.* **2011**, *13*, 593−603.
(50) Smith, J. D.; Cappa, C. D.; Wilson, K. R.; Messer, B. M.; Cohen, R. C.; Saykally, R. J. Energetics of hydrogen bond network rearrangements in liquid water. *Science* **2004**, *306*, 851−853.
(51) Wernet, P.; Nordlund, D.; Bergmann, U.; Cavalleri, M.; Odelius, M.; Ogasawara, H.; Näslund, L.-Å.; Hirsch, T. K.; Ojamäe, L.; Glatzel, P.; Pettersson, L. G. M.; Nilsson, A. The structure of the first coordination shell in liquid water. *Science* **2004**, *304*, 995−999.
(52) Huang, C.; Wikfeldt, K. T.; Tokushima, T.; Nordlund, D.; Harada, Y.; Bergmann, U.; Niebuhr, M.; Weiss, T. M.; Horikawa, Y.; Leetmaa, M.; Ljungberg, M. P.; Takahashi, O.; Lenz, A.; Ojamäe, L.; Lyubartsev, A. P.; Shin, S.; Pettersson, L. G. M.; Nilsson, A. The inhomogeneous structure of water at ambient conditions. *Proc. Natl. Acad. Sci. U. S. A.* **2009**, *106*, 15214−15218.
(53) Näslund, L.-Å.; Edwards, D. C.; Wernet, P.; Bergmann, U.; Ogasawara, H.; Pettersson, L. G. M.; Myneni, S.; Nilsson, A. X-ray absorption spectroscopy study of the hydrogen bond network in the bulk water of aqueous solutions. *J. Phys. Chem. A* **2005**, *109*, 5995−6002.
(54) Waluyo, I.; Huang, C.; Nordlund, D.; Weiss, T. M.; Pettersson, L. G. M.; Nilsson, A. Increased fraction of low-density structures in aqueous solutions of fluoride. *J. Chem. Phys.* **2011**, *134*, 224507.
(55) Wilson, K. R.; Cavalleri, M.; Rude, B. S.; Schaller, R. D.; Catalano, T.; Nilsson, A.; Saykally, R. J.; Pettersson, L. G. M. X-ray absorption spectroscopy of liquid methanol microjets: Bulk electronic structure and hydrogen bonding network. *J. Phys. Chem. B* **2005**, *109*, 10194−10203.
(56) Tamenori, Y.; Okada, K.; Takahashi, O.; Arakawa, S.; Tabayashi, K.; Hiraya, A.; Gejo, T.; Honma, K. Hydrogen bonding in methanol

clusters probed by inner-shell photoabsorption spectroscopy in the carbon and oxygen K-edge regions. *J. Chem. Phys.* **2008**, *128*, 124321.
(57) Guo, J.-H.; Luo, Y.; Augustsson, A.; Kashtanov, S.; Rubensson, J.-E.; Shuh, D. K.; Ågren, H.; Nordgren, J. Molecular structure of alcohol-water mixtures. *Phys. Rev. Lett.* **2003**, *91*, 157401.
(58) Kashtanov, S.; Augustsson, A.; Rubensson, J.-E.; Nordgren, J.; Ågren, H.; Guo, J.-H.; Luo, Y. Chemical and electronic structures of liquid methanol from X-ray emission spectroscopy and density functional theory. *Phys. Rev. B* **2005**, *71*, 104205.
(59) Nagasaka, M.; Hatsui, T.; Horigome, T.; Hamamura, Y.; Kosugi, N. Development of a liquid flow cell to measure soft X-ray absorption in transmission mode: A test for liquid water. *J. Electron Spectrosc. Relat. Phenom.* **2010**, *177*, 130−134.
(60) Hatsui, T.; Shigemasa, E.; Kosugi, N. Design of a transmission grating spectrometer and an undulator beamline for soft X-ray emission studies. *AIP Conf. Proc.* **2004**, *705*, 921−924.
(61) Nagasaka, M.; Yuzawa, H.; Horigome, T.; Hitchcock, A. P.; Kosugi, N. Electrochemical reaction of aqueous iron sulfate solutions studied by Fe L-edge soft X-ray absorption spectroscopy. *J. Phys. Chem. C* **2013**, *117*, 16343−16348.
(62) Chantler, C. T. Detailed tabulation of atomic form factors, photoelectric absorption and scattering cross section, and mass attenuation coefficients in the vicinity of absorption edges in the soft X-ray (Z = 30−36, Z = 60−89, E = 0.1 keV−10 keV), addressing convergence issues of earlier work. *J. Phys. Chem. Ref. Data* **2000**, *29*, 597−1048.
(63) Coreno, M.; de Simone, M.; Prince, K. C.; Richter, R.; Vondráček, M.; Avaldi, L.; Camilloni, R. Vibrationally resolved oxygen K → Π* spectra of O_2 and CO. *Chem. Phys. Lett.* **1999**, *306*, 269−274.
(64) Hempelmann, A.; Piancastelli, M. N.; Heiser, F.; Gessner, O.; Rüdel, A.; Becker, U. Resonant photofragmentation of methanol at the carbon and oxygen K-edge by high-resolution ion-yield spectroscopy. *J. Phys. B: At. Mol. Opt. Phys.* **1999**, *32*, 2677−2689.
(65) Prince, K. C.; Richter, R.; de Simone, M.; Alagia, M.; Coreno, M. Near edge X-ray absorption spectra of some small polyatomic molecules. *J. Phys. Chem. A* **2003**, *107*, 1955−1963.
(66) Hess, B.; Kutzner, C.; van der Spoel, D.; Lindahl, E. GROMACS 4: Algorithms for highly efficient, load-balanced, and scalable molecular simulation. *J. Chem. Theory Comput.* **2008**, *4*, 435−447.
(67) Jorgensen, W. L.; Tirado-Rives, J. Potential energy functions for atomic-level simulations of water and organic and biomolecular systems. *Proc. Natl. Acad. Sci. U. S. A.* **2005**, *102*, 6665−6670.
(68) Caleman, C.; Van Maaren, P. J.; Hong, M.; Hub, J. S.; Costa, L. T.; Van der Spoel, D. Force field benchmark of organic liquids: density, enthalpy of vaporization, heat capacities, surface tension, isothermal compressibility, volumetric expansion coefficient, and dielectric constant. *J. Chem. Theory Comput.* **2012**, *8*, 61−74.
(69) Mahoney, M. W.; Jorgensen, W. L. A five-site model for liquid water and the reproduction of the density anomaly by rigid, nonpolarizable potential functions. *J. Chem. Phys.* **2000**, *112*, 8910−8922.
(70) Nose, S. Constant-temperature molecular dynamics. *J. Phys.: Condens. Matter* **1990**, *2*, SA115−SA119.
(71) Parrinello, M.; Rahman, A. Polymorphic transitions in single crystals: A new molecular dynamics method. *J. Appl. Phys.* **1981**, *52*, 7182−7190.
(72) Darden, T.; York, D.; Pedersen, L. Particle mesh Ewald: An $N\bullet\log(N)$ method for Ewald sums in large systems. *J. Chem. Phys.* **1993**, *98*, 10089−10092.
(73) Matsumoto, M. Relevance of hydrogen bond definitions in liquid water. *J. Chem. Phys.* **2007**, *126*, 054503.